Molecular Medium

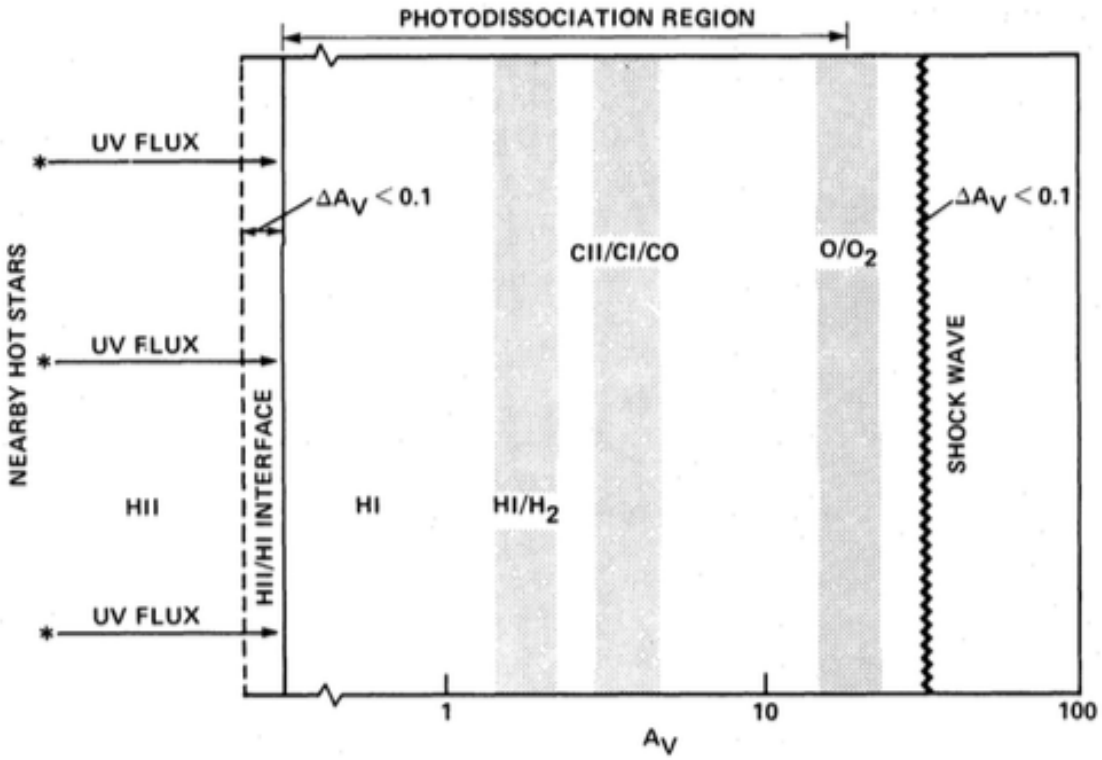

FIG. 1.—A schematic drawing of a photodissociation region. Our one-dimensional theoretical models extend from the predominantly atomic region to the point where O_2 is not appreciably photodissociated. Hence, the photodissociation region includes gas whose hydrogen is mostly H_2 and whose carbon is mostly in CO. The above diagram is roughly for Orion-like conditions with intense FUV fields incident upon the cloud. Large columns of warm O, C, C^+, and CO and vibrationally excited H_2 are produced in the photodissociation region.

Tielens & Hollenbach 1985

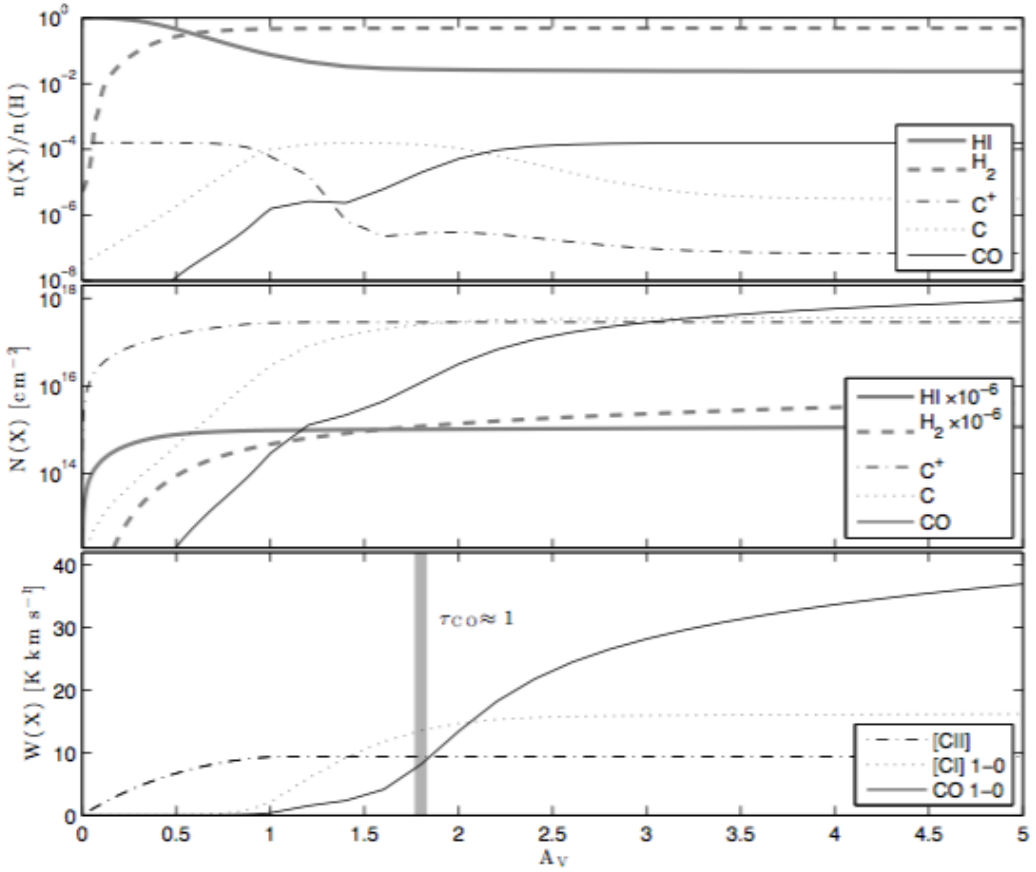

FIG. 1.— Calculated cloud structure as a function of optical depth into the cloud. Top panel shows the fractional abundance of HI, H_2, C^+, C, and CO. Middle panel shows their integrated column densities from the cloud edge. Bottom panel shows the emergent line intensity in units of K km s^{-1} for [CII] 158 μm, [CI] 609 μm, and CO $J = 1 \rightarrow 0$. The grey vertical bar shows where CO $J = 1 \rightarrow 0$ becomes optically thick. At the outer edge of the cloud gas is mainly HI. H_2 forms at $A_V \sim 0.5$ while the carbon is mainly C^+. The C^+ is converted to C at $A_V \sim 1$ and CO dominates at $A_V \gtrsim 2$. The model uses constant H density $n = 3 \times 10^3$ cm^{-3}, a radiation field $\chi = 30$ times the interstellar radiation field of Draine (1978), a primary cosmic-ray ionization rate of 2×10^{-16} s^{-1} per hydrogen nucleon, and are based on the PDR models of Wolfire, Hollenbach & McKee (2010) and Hollenbach et al. (2012).

Bolatto, Wolfire, & Leroy (2013)

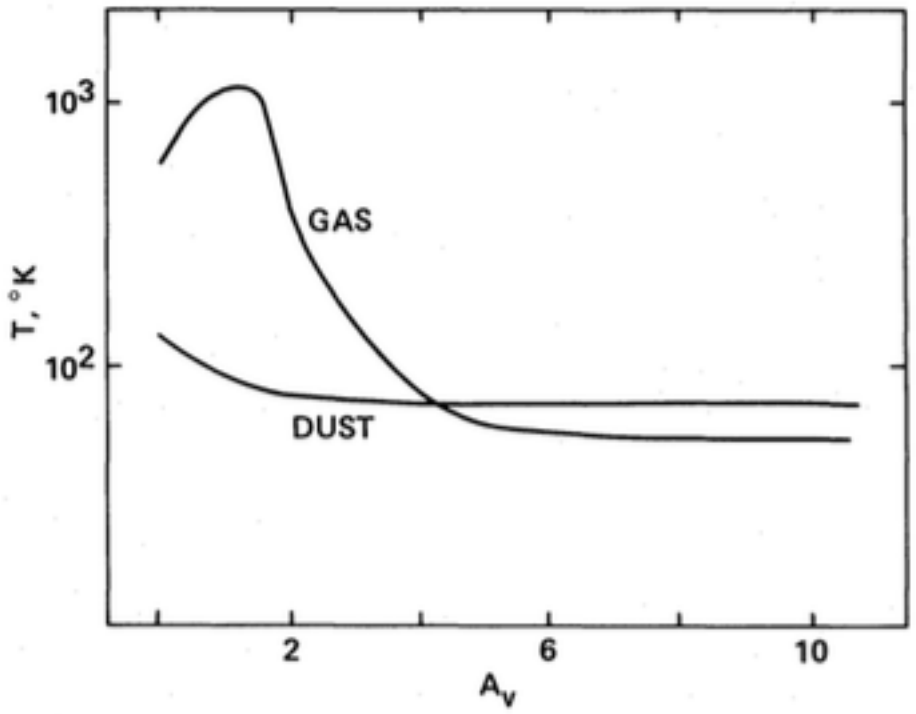

FIG. 7.—The calculated gas and dust temperature in the standard model is plotted as a function of the visual extinction A_v into the cloud.

Tielens & Hollenbach 1985

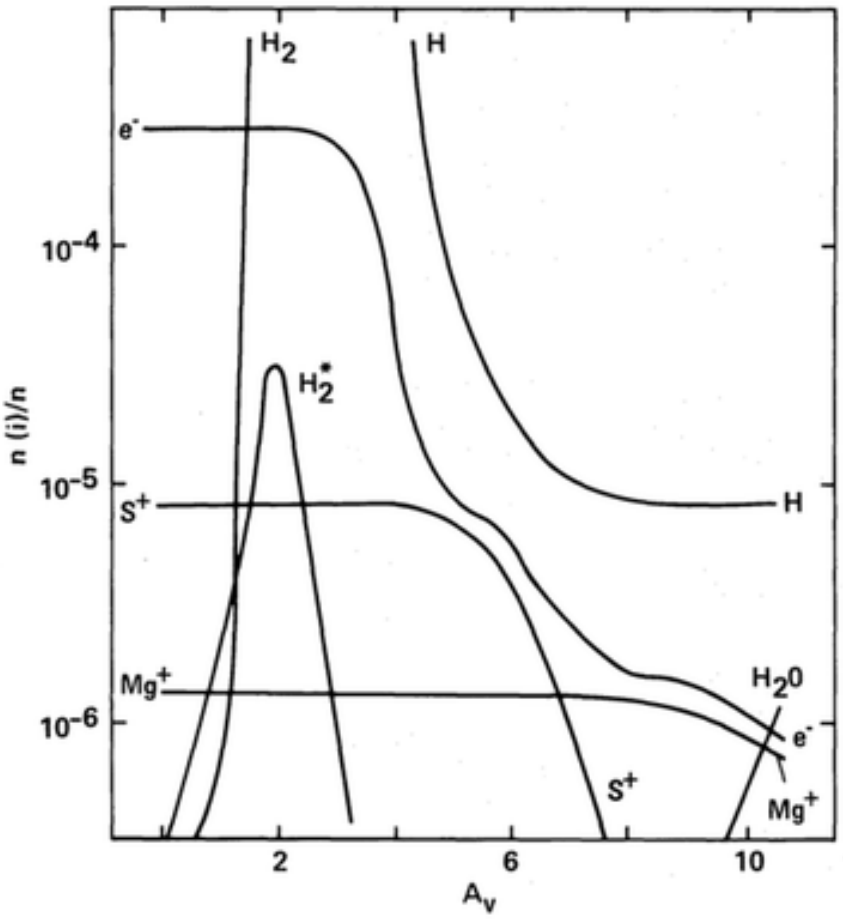

FIG. 9*a*

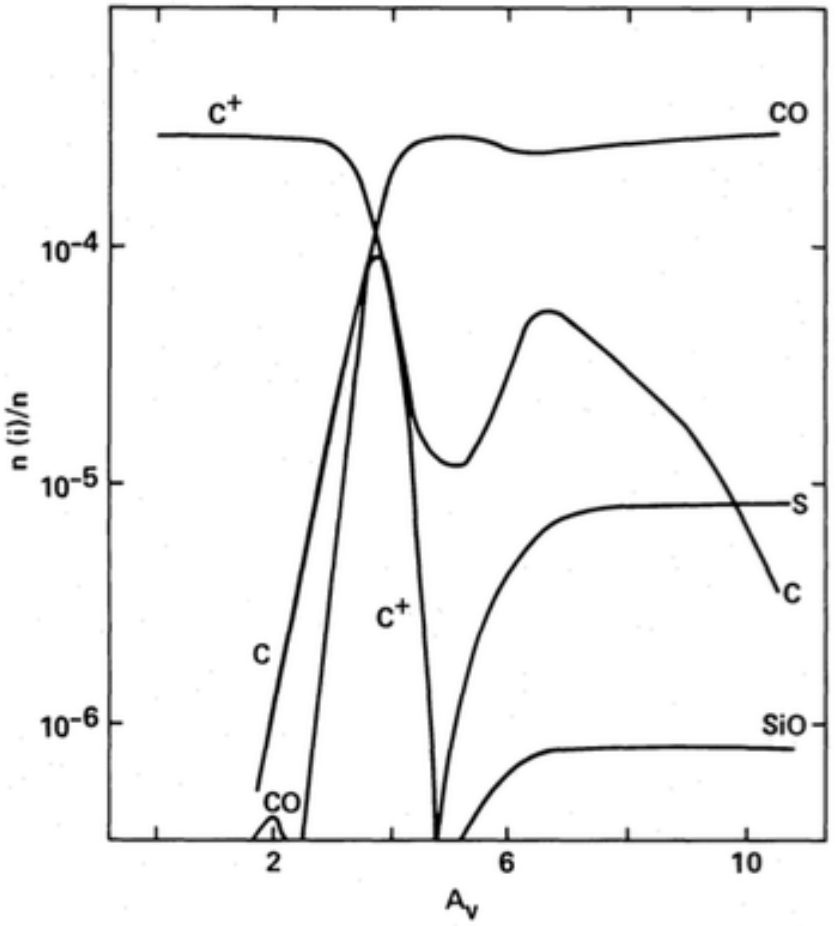

FIG. 9*b*

FIG. 9.—The molecular abundances of species i, $n(i)/n_0$, are plotted as a function of visual extinction A_v into the cloud for the standard model

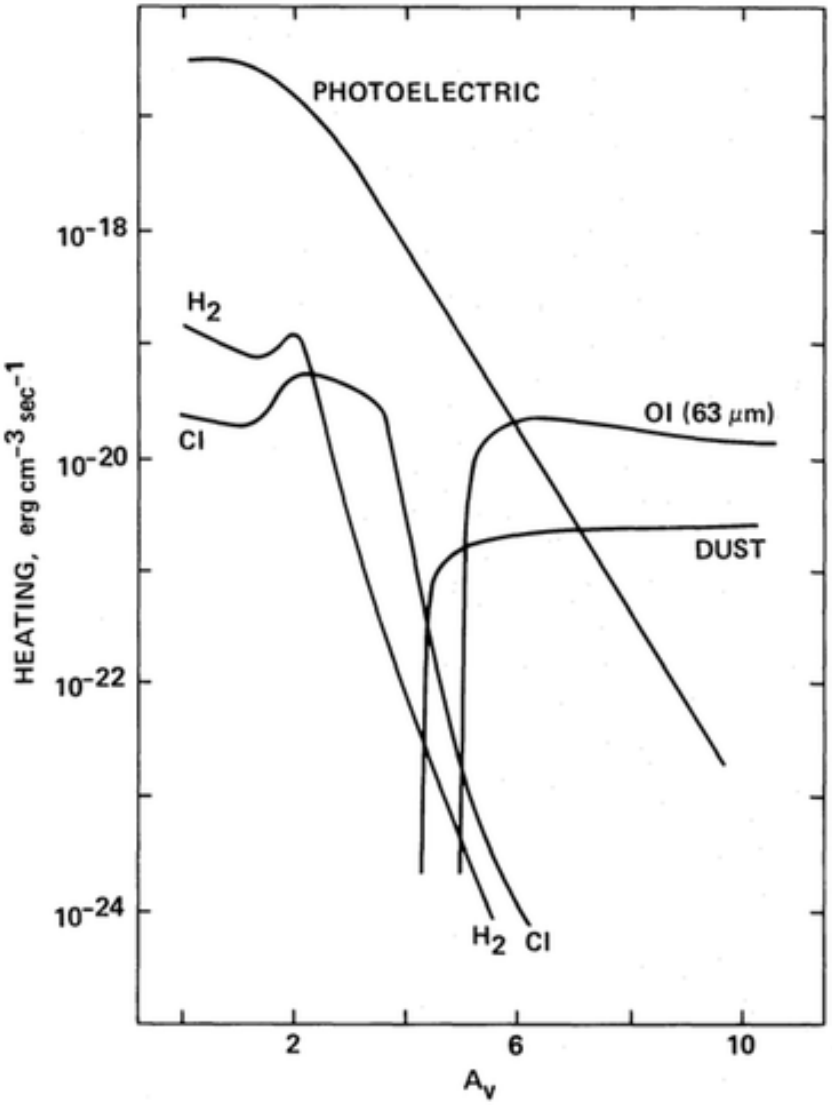

FIG. 8a

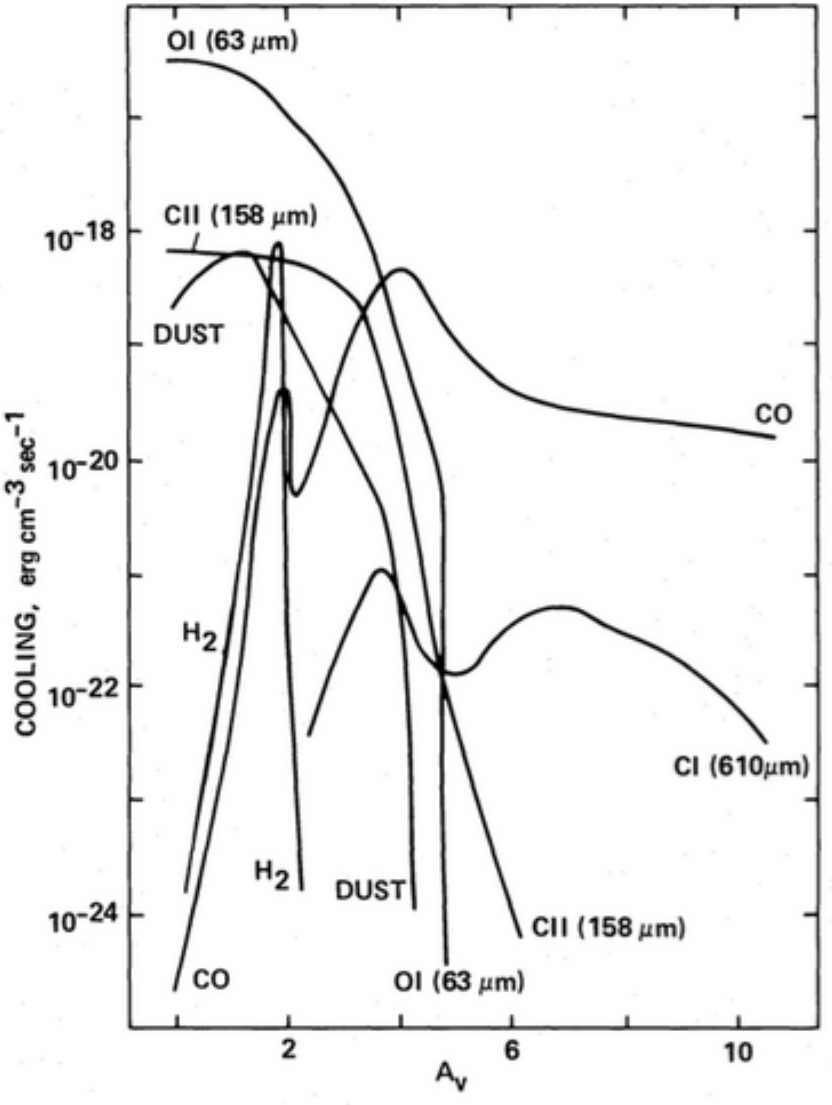

FIG. 8b

FIG. 8.—(*a*) The different heating terms in the energy balance are given as a function of visual extinction A_v into the cloud for the standard model (see text). (*b*) The different cooling terms in the energy balance are shown as a function of visual extinction A_v into the cloud for the standard model (see text).

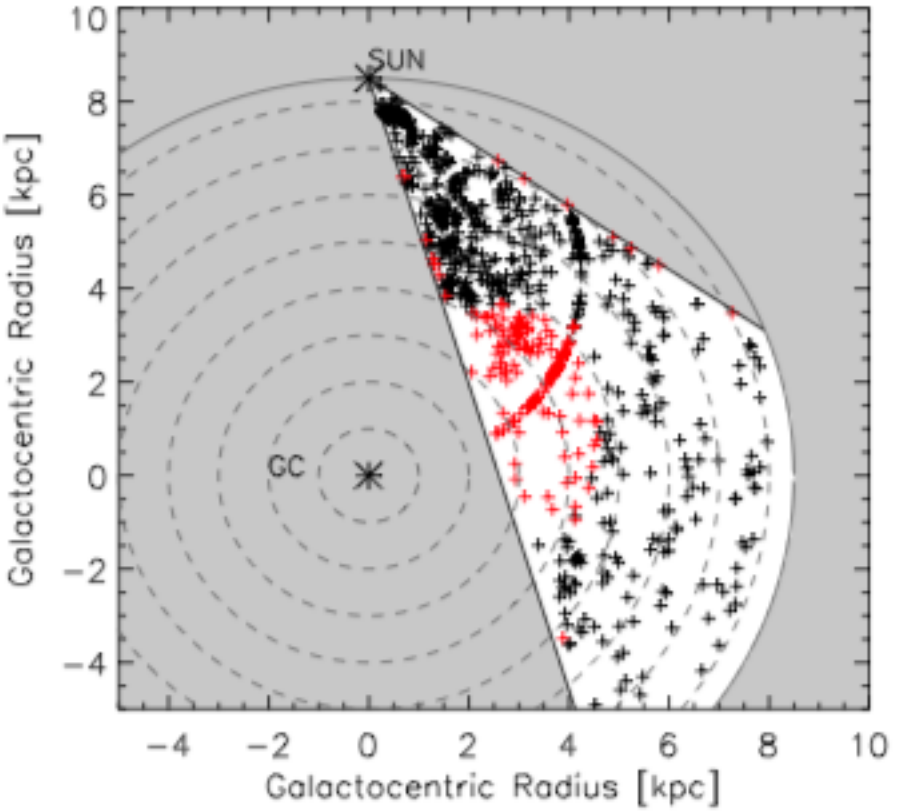

Figure 2. Positions of the GRS molecular clouds covered by the UMSB ^{12}CO survey (black crosses) and outside of the UMSB coverage (red crosses). The dashed circles indicate Galactocentric radii R_{gal} = 1–8 kpc, by steps of 1 kpc. The solid circle indicates the solar circle. The white area corresponds to the portion of the Galactic plane covered by the GRS. The artefact produced by the alignment of clouds in an arc of circle is due to the tangent point. Indeed, molecular clouds with radial velocities greater than the radial velocity of the tangent point (due to uncertainties in the rotation curve and non-circular motions) were assigned the distance of the tangent point.

Duval et al. (2010)

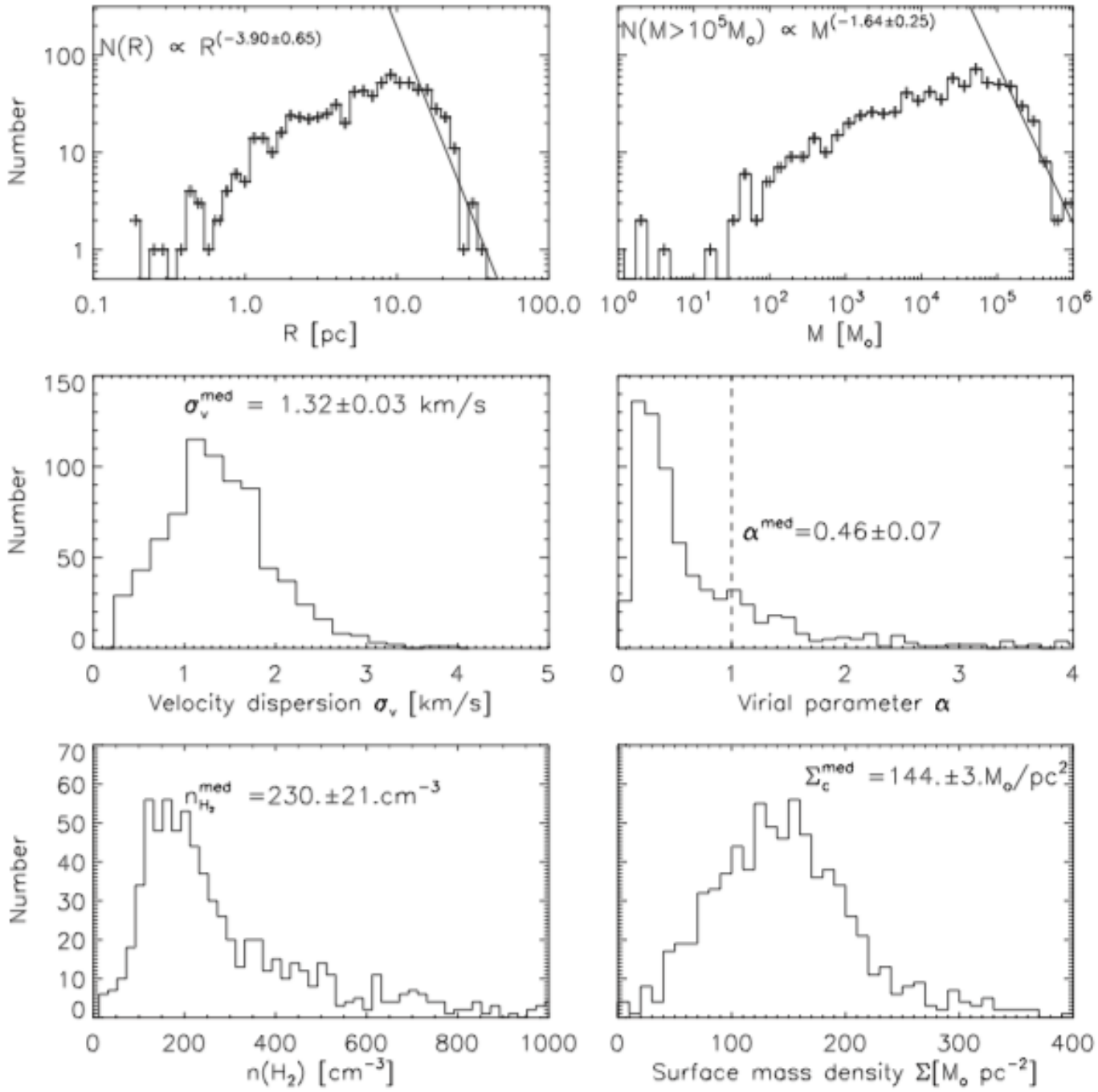

re 3. Histograms of the physical properties of molecular clouds. In the top two panels, the solid line indicates the best fit to the radius and mass spectra.

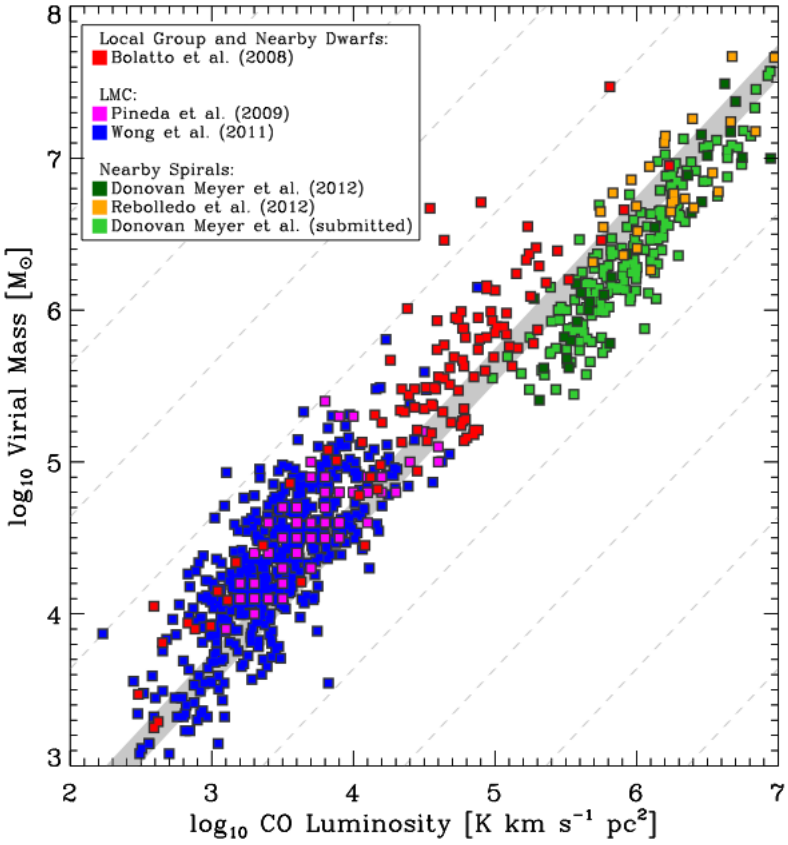

FIG. 6.— Relation between virial mass (y-axis) and CO luminosity (x-axis) for extragalactic GMCs. We show virial masses measured from selected high spatial resolution CO observations of nearby galaxies: the compilation of Bolatto et al. (2008, including M31, M33, and nine dwarf galaxies), high resolution studies of the LMC by Pineda et al. (2009) and Wong et al. (2011), and high resolution studies of the nearby spiral NGC 6946 by Donovan Meyer et al. (2012) and Rebolledo et al. (2012), as well as NGC 4826 and NGC 4736 by Donovan Meyer et al. (2013). Dashed lines show fixed $X_{\rm CO}$, with the typical Milky Way value $X_{\rm CO,20} = 2$ and $\pm 30\%$ indicated by the gray region. Virial mass correlates with luminosity, albeit with large scatter, across more than three orders of magnitude in extragalactic systems. The median across all displayed data is $X_{\rm CO,20} = 2.8$ with 0.4 dex scatter and the best fit relation has a power law index 0.90 ± 0.05, reflecting that most Local Group clouds show $X_{\rm CO,20} \sim 4$ while both studies of the bright spiral NGC 6946 find a lower $X_{\rm CO,20} \approx 1-2$.

Bolatto, Wolfire, & Leroy (2013)